

Si–O Bonded Interactions in Silicate Crystals and Molecules: A Comparison

G. V. Gibbs,^{*,†} D. Jayatilaka,[‡] M. A. Spackman,[‡] D. F. Cox,^{||} and K. M. Rosso[§]

Department of Geosciences, Materials Science and Engineering and Mathematics and Department of Chemical Engineering, Virginia Polytechnic Institute and State University, Blacksburg, Virginia 24061, School of Biomedical, Biomolecular, and Chemical Sciences, University of Western Australia, Perth, Australia, and William R. Wiley Environmental Molecular Sciences Laboratory, Pacific Northwest National Laboratories, Richland, Washington 99352

Received: June 21, 2006; In Final Form: September 21, 2006

Bond critical point, local kinetic energy density, $G(\mathbf{r}_c)$, and local potential energy density, $V(\mathbf{r}_c)$, properties of the electron density distributions, $\rho(\mathbf{r})$, calculated for silicates such as quartz and gas-phase molecules such as disiloxane are similar, indicating that the forces that govern the Si–O bonded interactions in silica are short-ranged and molecular-like. Using the $G(\mathbf{r}_c)/\rho(\mathbf{r}_c)$ ratio as a measure of bond character, the ratio increases as the Si–O bond length, the local electronic energy density, $H(\mathbf{r}_c) = G(\mathbf{r}_c) + V(\mathbf{r}_c)$, and the coordination number of the Si atom decrease and as the accumulation of the electron density at the bond critical point, $\rho(\mathbf{r}_c)$, and the Laplacian, $\nabla^2\rho(\mathbf{r}_c)$, increase. The $G(\mathbf{r}_c)/\rho(\mathbf{r}_c)$ and $H(\mathbf{r}_c)/\rho(\mathbf{r}_c)$ ratios categorize the bonded interaction as observed for other second row atom M–O bonds into discrete categories with the covalent character of each of the M–O bonds increasing with the $H(\mathbf{r}_c)/\rho(\mathbf{r}_c)$ ratio. The character of the bond is examined in terms of the large net atomic charges conferred on the Si atoms comprising disiloxane, stishovite, quartz, and forsterite and the domains of localized electron density along the Si–O bond vectors and on the reflex side of the Si–O–Si angle together with the close similarity of the Si–O bonded interactions observed for a variety of hydroxyacid silicate molecules and a large number of silicate crystals. The bond critical point and local energy density properties of the electron density distribution indicate that the bond is an intermediate interaction between Al–O and P–O bonded interactions rather than being a closed-shell or a shared interaction.

Introduction

The electron density distribution, $\rho(\mathbf{r})$, for a material strives to adopt a configuration wherein the forces on the atoms are zero, and the energy of the resulting configuration is minimized. When these conditions prevail, the distribution embodies the bulk of the information about the system, including its structure, bonded interactions, and sites of potential chemical activity.¹ In an effort to retrieve this information, Bader and co-workers² forged a theory that pictures a material as a network of interacting atoms with the bonded atoms connected by pathways of electron density. Within this framework, they found that the interactions can be characterized by a set of well-defined bond critical point and local energy density properties measured at stationary points in $\rho(\mathbf{r})$, where $\nabla\rho(\mathbf{r}) = 0$ and $\rho(\mathbf{r})$ adopts a local minimum value. The properties were not only found to serve as a basis for determining whether a pair of atoms is bonded, but they were also found to provide a basis for classifying the bonded interactions. The theory also provided strategies for making a quantitative comparison of the bonded interactions displayed by a variety of systems including molecules and crystals.

The theory will be used in this study to clarify our understanding of the properties of the Si–O bonded interactions comprising molecules and crystals by addressing such questions

as (1) why can gas-phase molecules such as disiloxane, $\text{H}_3\text{SiOSiH}_3$, be successfully used as model structures in the geosciences to advance our understanding of the reaction of the silica polymorph quartz, for example, with water and related molecules at the atomic level?^{3–7} and (2) why can the force field and the structure of the tiny hydroxyacid silicate molecule $(\text{OH})_3\text{Si–O–Si}(\text{OH})_3$ be used successfully to generate the structures of more than 1400 structure types for crystalline silica, including quartz and cristobalite?^{8,9} In addressing these questions, the properties of $\rho(\mathbf{r})$ calculated for the Si–O bonded interactions observed for a large number of silicate crystals, including the silica polymorphs, will be compared with those calculated for a variety of hydroxyacid silicate molecules. The comparison will indicate that the properties of the electron density distributions for the Si–O bonded interactions for molecules and crystals are similar, suggesting that the bond energies are similar. On the basis of the agreement, it is concluded that the properties of the Si–O bonded interactions in molecules and crystalline silica are similar, providing an experimental and theoretical basis for clarifying why model representative silicate molecules can be successfully used in the study of the structure, the emission spectra, the critical point properties, and the dissolution of Earth materials.^{10,11}

The properties of the bond will also be examined with the goal of clarifying whether the bonded interactions comprising an SiO_4 silicate tetrahedral oxyanion in quartz with four-coordinated Si have a greater shared character than those that comprise an SiO_6 octahedral oxyanion in stishovite with six-coordinated Si. In several earlier studies of bonded interactions, it was demonstrated that the covalent character of an M–X bond

* Corresponding author. Phone: (540) 231-6330. Fax: (540) 231-5022. E-mail: gvgibbs@vt.edu.

[†] Department of Geosciences, Materials Science and Engineering and Mathematics, Virginia Tech.

[‡] University of Western Australia.

^{||} Department of Chemical Engineering, Virginia Tech.

[§] Pacific Northwest National Laboratories.

increases as the coordination number of the M atom decreases for a large variety of M_iX_j ($i, j = 1, 2, \text{ or } 3$; $M = \text{Na, Mg, Ca, Si, etc.}$; and $Y = \text{F, Cl, O, S, etc.}$) solid-state materials.^{12,13} In general, it was found that the smaller the coordination number, ν_M , of the M atom, the more covalent and the more directed the M–X bond vectors and conversely, the larger the value of ν_M , the more ionic and the less directed the bond vectors. Our study will show that a similar connection exists between the covalent character of the Si–O bond and the coordination number of the Si atom, ν_{Si} .

Despite the great abundance of silica in nature (comprising 45% of the Earth's crust and mantle¹⁴), and the importance of SiO_2 and the Si– SiO_2 interfaces in physics and chemistry, the nature of the Si–O bond has eluded a universally accepted classification, being considered as strongly ionic by some,^{15,16} or intermediate,^{17,18} substantially covalent,^{19,20} or covalent by others.²¹ With the goal of advancing our understanding of its properties and the connection between the bonded interactions in molecules and crystals, the bond critical point and local energy density properties for a number of silicate crystals will be compared with those calculated for a variety of representative hydroxyacid silicate molecules. The comparison will suggest that the Si–O bonded interaction is intermediate with the shared character of the bonded interaction increasing with the local electronic energy density and the accumulation of electron density in the internuclear region.¹⁸

Bond Critical Point Properties

According to Bader and his colleagues,¹ a bonded interaction is defined to exist between a pair of atoms only if the pair is connected by a line of maximum electron density in $\rho(\mathbf{r})$, denoted the bond path, with a saddle point along the path at a stationary bond critical point, \mathbf{r}_c , where $\nabla\mathbf{r}(\mathbf{r}) = 0$. The assertion is made that a pair is considered to be bonded in a chemical sense only if they are connected by such a path and the path is mirrored along a similar path of maximally negative potential energy density linking the pair.²² The electron density along the path at \mathbf{r}_c is at a minimum value with respect to any displacement parallel to the path but a maximum with respect to any radial displacement perpendicular to the path. The value of $\rho(\mathbf{r}_c)$ has been observed to be a direct measure of the strength of a given metal oxygen M–O bond; the greater the value of $\rho(\mathbf{r}_c)$, typically the shorter the bond.²³ The trace of the Hessian of $\rho(\mathbf{r})$, $H_{ij} = \partial^2\rho(\mathbf{r})/\partial x_i\partial x_j$, when evaluated at \mathbf{r}_c and diagonalized equals the sum of eigenvalues $\lambda_1 + \lambda_2 + \lambda_3 = \nabla^2\rho(\mathbf{r}_c)$. The positive eigenvalue λ_3 for the Hessian defines the positive curvature of $\rho(\mathbf{r}_c)$ along the bond path, and the two eigenvalues λ_1 and λ_2 define the negative curvatures of $\rho(\mathbf{r}_c)$ perpendicular to the path. As the magnitudes of the three curvatures and the value of $\rho(\mathbf{r}_c)$ each increase, the length of a given M–O bond usually decreases in a regular way as electron density is accumulated and locally concentrated in the internuclear region between a pair of atoms.²³ Further, the local kinetic and potential energy densities each increase in magnitude at \mathbf{r}_c as the magnitudes of the curvatures each increase.

The sign of the Laplacian, $\nabla^2\rho(\mathbf{r}_c) = 4(2G(\mathbf{r}_c) + V(\mathbf{r}_c))$, determines whether the local potential energy density, $V(\mathbf{r}_c)$, or the local kinetic energy density, $G(\mathbf{r}_c)$, dominates at \mathbf{r}_c ¹ where $G(\mathbf{r}_c)$ is always positive and $V(\mathbf{r}_c)$ is always negative for a geometry optimized minimum energy structure. When $|V(\mathbf{r}_c)| > 2G(\mathbf{r}_c)$, $\nabla^2\rho(\mathbf{r}_c)$ is negative, $\rho(\mathbf{r}_c)$ is relatively large in value, and electron density is locally concentrated at \mathbf{r}_c , the bond is indicated to be a shared interaction, whereas when $2G(\mathbf{r}_c) > |V(\mathbf{r}_c)|$ and $\nabla^2\rho(\mathbf{r}_c)$ are positive, $\rho(\mathbf{r}_c)$ is relatively small, and

the electron density is locally depleted at \mathbf{r}_c , the bond is indicated to be either a closed-shell or a bond of intermediate character, depending on the location of \mathbf{r}_c relative to the nodal surface of the $\nabla^2\rho(\mathbf{r}_c)$.^{1,24} When \mathbf{r}_c is in close proximity with the surface, the bond is indicated to be an intermediate interaction, but when it is distant from the surface, the bond is indicated to be a closed-shell interaction; the greater the distance, the more closed-shell the interaction.²⁴

In contrast, Cremer and Kraka²⁵ classify bonded interactions on the basis of the sign of the local electronic energy density, $H(\mathbf{r}_c) = G(\mathbf{r}_c) + V(\mathbf{r}_c)$. When $|V(\mathbf{r}_c)| > G(\mathbf{r}_c)$ such that $H(\mathbf{r}_c)$ is negative and the value of $\rho(\mathbf{r}_c)$ is relatively large, a bond is indicated to be a shared interaction in that the electron density at \mathbf{r}_c is considered to have a stabilizing impact on the structure of a material. Conversely, when $G(\mathbf{r}_c) > |V(\mathbf{r}_c)|$ such that $H(\mathbf{r}_c)$ is positive and $\rho(\mathbf{r}_c)$ is relatively small, the bond is indicated to be a closed-shell interaction. In this case, the electron density at \mathbf{r}_c is considered to have a destabilizing impact on the material. Moreover, as $H(\mathbf{r}_c)$ decreases and $\rho(\mathbf{r}_c)$ increases in value for a given bonded interaction, the shared character of the interaction is indicated to increase as well.

More recently, Espinosa et al.²⁶ proposed a third classification based on the $|V(\mathbf{r}_c)|/G(\mathbf{r}_c)$ ratio rather than on signs and magnitudes of $\nabla^2\rho(\mathbf{r}_c)$ and $H(\mathbf{r}_c)$. They assume that a bond is a closed-shell interaction when $H(\mathbf{r}_c) \geq 0$ and that it is a shared interaction when $\nabla^2\rho(\mathbf{r}_c) \leq 0$. For the case where $H(\mathbf{r}_c) = 0$, $G(\mathbf{r}_c) + V(\mathbf{r}_c) = 0$ and $|V(\mathbf{r}_c)|/G(\mathbf{r}_c) = 1$. For the case where $\nabla^2\rho(\mathbf{r}_c) = 0$, $2G(\mathbf{r}_c) + V(\mathbf{r}_c) = 0$ and $|V(\mathbf{r}_c)|/G(\mathbf{r}_c) = 2$. With these equalities, a bonded interaction is asserted to be a closed-shell interaction when the ratio $|V(\mathbf{r}_c)|/G(\mathbf{r}_c) < 1$, a shared interaction when $|V(\mathbf{r}_c)|/G(\mathbf{r}_c) > 2$, and an intermediate interaction is asserted when the ratio falls in the interval between 1 and 2. Thus, the greater the value of $|V(\mathbf{r}_c)|/G(\mathbf{r}_c)$, the more there is a shared bonded interaction.

Si–O Bonded Interactions of Hydroxyacid Silicate Molecules and Silicate Crystals

Using a relatively robust BLYP/6-311G(2d,p) basis set and level of theory, Gibbs et al.²⁷ optimized the bond lengths and angles for more than a dozen hydroxyacid silicate molecules including molecules with SiO_4 , SiO_6 , and SiO_8 coordination polyhedra with four-, six-, and eight-coordinated Si atoms, respectively. Using the software EXTREME, kindly donated by Prof. Richard Bader, the Si–O bond critical point and the local electronic energy density properties $H(\mathbf{r}_c)$ for the molecules were evaluated. The resulting bcp properties were found to correlate with Si–O bond lengths, $R(\text{Si–O})$. As $\rho(\mathbf{r}_c)$, λ_3 , and $\nabla^2\rho(\mathbf{r}_c)$ each increase and as the bonded radius of the O atom, $r_b(\text{O})$, and λ_1 and λ_2 each decrease, the length of the Si–O bond decreases as $\rho(\mathbf{r})$ is progressively localized at \mathbf{r}_c and progressively locally concentrated perpendicular to the bond path and in the direction of the bonded atoms, progressively shielding the nuclei of the Si and O atoms.^{27–29} Unlike the other trends, those displayed by $R(\text{Si–O})$ versus $\rho(\mathbf{r}_c)$, λ_3 , and $\nabla^2\rho(\mathbf{r}_c)$ appear to depart from linearity, suggesting a nonlinear power law-like relationship. Also, $G(\mathbf{r}_c)$ increases while $V(\mathbf{r}_c)$ and $H(\mathbf{r}_c)$ are both negative and decrease nonlinearly as $R(\text{Si–O})$ decreases.

As observed previously, when the Laplacian is positive, a bond is classified as either a closed-shell or an intermediate interaction, depending on the proximity of \mathbf{r}_c with the nodal surface of the Laplacian distribution.²⁴ In the case of the hydroxyacid silicate molecules, \mathbf{r}_c was observed to move in succession in the direction of the nodal surface of the Si atom as ν_{Si} decreased from 8 to 6 to 4 with \mathbf{r}_c advancing from 0.65

Å to a distance of 0.15 Å from the surface for the four-coordinated Si atom for the (OH)₃Si–O–Si(OH)₃ molecule.^{27,29} Accordingly, the Si–O bond for the molecule is indicated to be of intermediate character, while that for the H₈SiO₆ molecule with six-coordinated Si is indicated to be a more closed-shell interaction and that for the H₁₂SiO₈ molecule with eight-coordinated Si is indicated to have an even greater closed-shell character. The observation that the experimental atomic basin charge for the six-coordinated Si atom for stishovite³⁰ is larger (+3.39 e) than that (+3.17 e) for the four-coordinate Si atom for forsterite³¹ and for quartz (+3.20 e)¹⁸ lends support to the connection between bond character and ν_{Si} . It is also consistent with trends established between Si–O bond length and ionicity with the substantially longer bond lengths in stishovite involving the Si atom with the largest net charge.³²

However, on the basis of these large net atomic charges, it would appear that the Si–O bond has a substantial component of closed-shell character. Indeed, Gillespie and Johnson¹⁶ have concluded that the bond comprising the H₃Si–O–SiH₃ molecule is a highly ionic bond with net atomic charges conferred on Si and O of +3.02 and –1.72 e, respectively. Given the small bending force constant of the Si–O–Si angle, ~5 N/m, calculated for the (OH)₃Si–O–Si(OH)₃ molecule,²³ together with a large net atomic charge on Si, it is difficult to reconcile why the angle observed for the molecule is bent at 144°, as observed for cristobalite,¹⁸ rather than straight if the bond is a closed-shell interaction and the charges on the Si atoms are large. Further, it is also notable that Cohen,¹⁵ in a first principles study of crystalline silica, concluded that “SiO₂ is held together by a combination of covalent sp σ bonding and ionic bonding between the highly charged tetravalent Si⁴⁺ and O²⁻ ions”. In contrast, the net atomic charges determined for the P atoms comprising the PO₄ tetrahedra and the Al atoms comprising the AlO₆ octahedra in the AlPO₄–15 molecular sieve were found to be +3.47 and +2.42 e, respectively.³³ Further, net charges calculated at the BLYP/6-311++(df,p) level for the molecules H₃PO₄ and H₂SO₄ are +3.59 and +3.85 e, respectively. Given the relatively large charges generated in these studies and calculations, it is not clear what significance and meaning should be attached to their magnitudes as they relate to the nature of the bonded interactions.^{34–39} Nonetheless, it is apparent that the magnitudes of the charges increase systematically from left to right in the periodic table from Al to S as the number of valence electrons and the electronegativities of the atoms increase.

According to the Cremer and Kraka²⁵ classification, the Si–O bonded interaction is indicated not only to be a shared interaction, as asserted by Harrison,²¹ but that the shared character is indicated to increase as ν_{Si} decreases from 8 to 6 to 4, $\rho(\mathbf{r}_c)$ increases systematically from 0.489 to 0.801 to 0.987 e/Å³, and $H(\mathbf{r}_c)$ decreases from –0.035 to –0.058 to –0.071 au, respectively.⁴⁰

The bcp properties for more than 125 Si–O bonded interactions have been calculated in a study of the bonded interactions for a wide variety of silicate crystals^{23,40} with the programs CRYSTAL98⁴¹ and TOPOND.⁴² As observed for the silicate molecules, as R(Si–O) decreases, $\rho(\mathbf{r}_c)$, λ_3 , and $\nabla^2\rho(\mathbf{r}_c)$ each increase and $\mathbf{r}_b(\text{O})$, λ_1 , and λ_2 decrease in value. It is evident that the trends displayed by the bcp properties for the crystals are similar to those displayed by the hydroxyacid silicate molecules. The trends differ, however, in that gaps exist in the scatter diagrams for the molecules where the number of Si–O bonded interactions for the molecules is far fewer than those observed for the crystals. The R(Si–O) versus $\mathbf{r}_b(\text{O})$ trend is linear as observed for the molecules, but the remaining trends

appear to be nonlinear as observed for several of the scatter diagrams displayed by the molecules.

Accurate single-crystal diffraction data, measured for the silica polymorphs stishovite and coesite, have been examined using multipole model refinement strategies.^{30,43} The Si–O bcp properties generated for the multipole model representations of the experimental electron density for the two polymorphs were found to be in close agreement with those calculated for the silicate crystals, affording support for the accuracy of the experimental data. The agreement between the theoretical and the experimental bcp properties serves to support the assertion that the properties generated with computational quantum methods rival the accuracy of those determined experimentally.^{31,43} It is notable that the values of $\rho(\mathbf{r}_c)$ observed for the Si–O bonds for the two silica polymorphs coesite and stishovite are in a fortuitous one-to-one correspondence with the Pauling⁴⁴ bond strengths, s . For example, the average value observed for the Si–O bonds of coesite (0.998 e/Å³) with four-coordinate Si matches the Pauling bond strength of $s = 1.0$. Also, the average value observed for the Si–O bonds for stishovite (0.663 e/Å³) with six-coordinate Si likewise matches the Pauling bond strength of $s = 2/3$.

The Si–O bond lengths and bcp properties calculated for the silicate molecules are compared with those calculated for the silicate crystals in Figure 1. The molecular data scatter close to the trends defined by the crystals, and the agreement of the bcp properties is credible evidence that the electron density distributions and the properties of the crystals and molecules are similar. Further, it supports the statement by Stewart and Spackman⁴⁵ that a quartz crystal can be viewed as a giant complex molecule, linked together by the same forces that link the Si–O–Si atoms together in a small gas-phase molecule like H₃SiOSiH₃. As observed by Gibbs,¹⁰ the end result is a set of experimental bond lengths and angles (R(Si–O) = 1.640 Å and $\angle\text{SiOSi} = 144^\circ$) for the gas-phase molecule⁴⁶ and for the molecular crystal⁴⁷ (R(Si–O) = 1.640 Å and $\angle\text{SiOSi} = 142^\circ$) that match those observed for a quartz crystal (R(Si–O) = 1.610 Å and $\angle\text{SiOSi} = 144^\circ$). In short, the close similarity of the Si–O bond lengths and Si–O–Si angles and the electron density distributions for a quartz crystal and a gas-phase molecule like H₃SiOSiH₃ implies that the forces that govern the two structures are short ranged and molecular-like. Also, the bond lengths and angles observed for a relatively large number of silica polymorphs such as quartz have been shown to conform closely with a potential energy surface calculated for the (OH)₃SiOSi(OH)₃ molecule,²³ again suggesting that the forces that govern the energy of the Si–O bond, Si–O bond lengths, and Si–O–Si angles are molecular-like.

Local Energy Density Properties for the Si–O Bonded Interactions Comprising Silicate Crystals and Molecules

A recent analysis of the M–O bonded interactions for the silicates considered in this study and other earth materials shows that the $G(\mathbf{r}_c)/\rho(\mathbf{r}_c)$ ratio correlates with bond length with the ratio increasing as ν_{M} and R(M–O) both decrease, as $\rho(\mathbf{r}_c)$ increases, and as $H(\mathbf{r}_c)$ becomes progressively more negative.⁴⁸ In other words, the ratio appears to be a direct measure of the strength and covalent character of a given M–O bond; the larger the ratio, the more covalent the bond. Combined, the $G(\mathbf{r}_c)/\rho(\mathbf{r}_c)$ and $H(\mathbf{r}_c)/\rho(\mathbf{r}_c)$ ratios were also found to categorize the M–O bond data into distinct categories with the shared character of the M–O bonds increasing as $H(\mathbf{r}_c)/\rho(\mathbf{r}_c)$ decreases. A scatter diagram of the $G(\mathbf{r}_c)/\rho(\mathbf{r}_c)$ and $H(\mathbf{r}_c)/\rho(\mathbf{r}_c)$ ratios is displayed in Figure 2 for the second row Na–O, Mg–O, Al–O, Si–O,

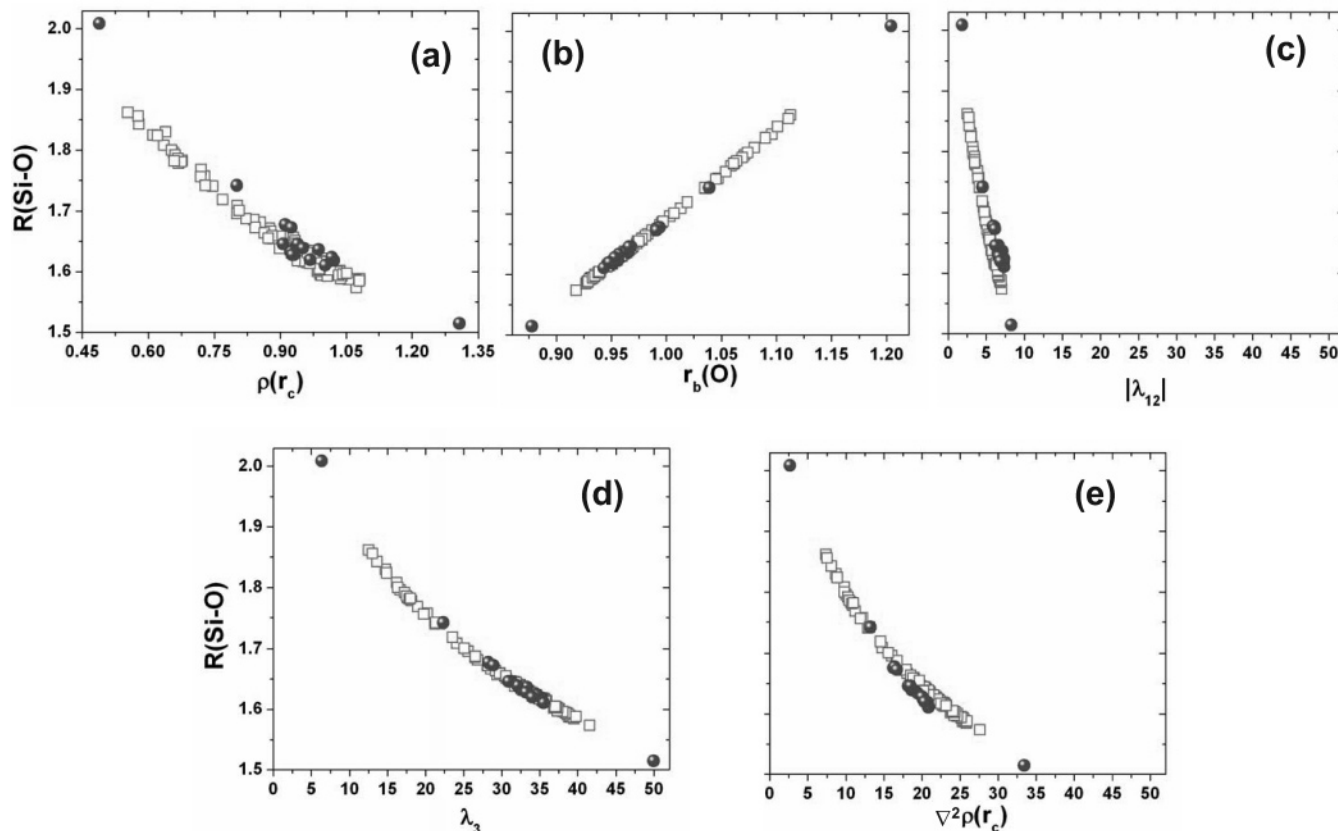


Figure 1. Scatter diagrams of the bond critical point (bcp) properties plotted against the experimental bond lengths, $R(\text{Si-O})$ (squares), for a relatively larger number of silicate crystals:²³ (a) $R(\text{Si-O})$ vs $\rho(\mathbf{r}_c)$, the value of the electron density, ρ , at the bond critical point, \mathbf{r}_c ; (b) $R(\text{Si-O})$ vs $r_b(\text{O})$, the bonded radius of the O atom; (c) $R(\text{Si-O})$ vs $|\lambda_{12}|$, where $\lambda_{12} = 1/2(\lambda_1 + \lambda_2)$ and $\lambda_1 + \lambda_2$ measure the negative curvatures of ρ perpendicular to the bond path at \mathbf{r}_c ; (d) $R(\text{Si-O})$ vs λ_3 , the positive curvature of ρ measured parallel to the bond path at \mathbf{r}_c ; and (e) $R(\text{Si-O})$ vs $\nabla^2\rho(\mathbf{r}_c)$, the Laplacian of ρ measured at \mathbf{r}_c . Superimposed on each diagram are the bcp properties (spheres) calculated for a variety of geometry optimized molecules containing Si–O bonds.²⁷ In preparing these plots, it was discovered that the bcp properties for the $\text{H}_3\text{Si-O-SiH}_3$ molecule were incorrectly reported in Table 1 of ref 27. They should read $\rho(\mathbf{r}_c) = 0.906 \text{ e}/\text{\AA}^3$, $r_b(\text{O}) = 0.966 \text{ \AA}$, $\lambda_{12} = -6.212 \text{ e}/\text{\AA}^5$, $\lambda_3 = 30.88 \text{ e}/\text{\AA}^5$, $\nabla^2\rho(\mathbf{r}_c) = 14.46 \text{ e}/\text{\AA}^5$, and $H(\mathbf{r}_c) = 0.238 \text{ au}/\text{\AA}^3$.

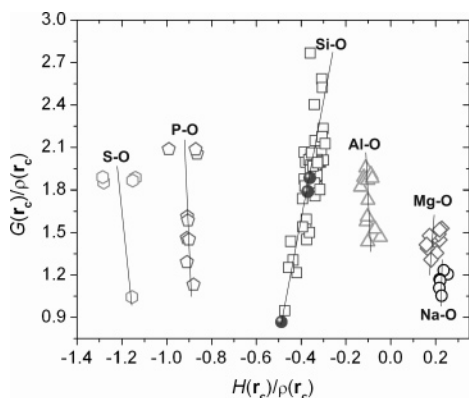


Figure 2. Scatter diagram of $G(\mathbf{r}_c)/\rho(\mathbf{r}_c)$ vs $V(\mathbf{r}_c)/\rho(\mathbf{r}_c)$ for second row M–O bonded interactions for Earth materials (open symbols) where $G(\mathbf{r}_c)$ is the local kinetic energy density, $H(\mathbf{r}_c) = G(\mathbf{r}_c) + V(\mathbf{r}_c)$ is the local electronic energy density, and $\rho(\mathbf{r}_c)$ is the value of the electron density, each evaluated at \mathbf{r}_c . The figure was adapted from Figure 4 in ref 48. Plotted as spheres along the Si–O data trend are the $G(\mathbf{r}_c)/\rho(\mathbf{r}_c)$ vs $V(\mathbf{r}_c)/\rho(\mathbf{r}_c)$ values calculated for $\text{H}_{12}\text{SiO}_8$, $\text{H}_{12}\text{SiO}_6$, and H_4SiO_4 molecules with ν_{Si} increasing from 8 to 6 to 4 from the bottom upward.

P–O, and S–O bonds observed for the Earth materials. It is apparent that these ratios categorize the data into discrete domains with $H(\mathbf{r}_c)/\rho(\mathbf{r}_c)$ becoming more negative from right to left in the figure as the electronegativities of the M atoms increase. Further, the shared character of the M–O bonds is

indicated to increase with the increasing value of $G(\mathbf{r}_c)/\rho(\mathbf{r}_c)$ as observed above. With the location of the Si–O bond data between the Al–O and P–O data, we are inclined to classify the Si–O as a bond of intermediate character rather than either closed-shell or shared as done earlier on the basis of the bcp properties.¹⁸

The values of $G(\mathbf{r}_c)$ and $V(\mathbf{r}_c)$ were not recorded in the earlier study of the hydroxyacid silicate molecules. However, for purposes of comparison, the geometries of the molecules H_4SiO_4 (S_4), H_8SiO_6 (O_h), and $\text{H}_{12}\text{SiO}_8$ (O_h) were optimized for this study at the BLYP/6-311++(df,p) level, and their $G(\mathbf{r}_c)$, $V(\mathbf{r}_c)$, and $\rho(\mathbf{r}_c)$ values were evaluated. The $G(\mathbf{r}_c)/\rho(\mathbf{r}_c)$ and $H(\mathbf{r}_c)/\rho(\mathbf{r}_c)$ values for the molecules were added to Figure 2 in a comparison with those displayed for the crystals. Clearly, the molecular data fall well within the trend displayed by the data for the silicates, indicating that the local kinetic and potential energy densities for the molecules and crystals are similar and further evidence that the bonded interactions in a silicate crystal are molecular-like. However, the $G(\mathbf{r}_c)/\rho(\mathbf{r}_c)$ ratios calculated for the molecules are somewhat smaller than those displayed by the crystals. Also, as observed for the crystals, ν_{Si} increases as $H(\mathbf{r}_c)$ decreases and $G(\mathbf{r}_c)/\rho(\mathbf{r}_c)$ increases, indicating that the covalent (shared) character of the Si–O bond increases with decreasing coordination number in agreement with the trends established earlier by Mooser and Pearson¹² and Phillips.¹³ When an array of separated atoms coalesce into a stable bonded array, $G(\mathbf{r})$ increases while $V(\mathbf{r})$ decreases, the end result being

a negative $H(\mathbf{r}_c)$ value for a shared interaction, resulting in the stabilization of the array.²⁵ The similarity of the $H(\mathbf{r}_c)$ and $\rho(\mathbf{r}_c)$ values for the molecules and crystals indicates that the accumulation of the electron density at the bond critical points has a similar impact on the stabilization of their structures.

Conclusion

As we have seen, the character of the Si–O bonded interaction has eluded a universally accepted classification with the bond being classified as either a closed-shell, a shared, or an intermediate interaction.^{16,19–21} The large net atomic charges calculated for the Si atoms for the $\text{H}_3\text{SiOSiH}_3$ molecule, those observed for stishovite and forsterite, and those calculated for quartz indicate that the interaction is a closed-shell interaction. In contrast, the proximity of \mathbf{r}_c to the nodal plane of the Laplacian indicates that it is an intermediate interaction. Further, the Si–O–Si bonded interactions for the silica polymorph coesite display well-developed bond electron pair domains along the Si–O bond vectors and well-developed nonbonded electron pair domains on the reflex side of the Si–O–Si angle, features expected for a bond with a component of shared character.^{43,49} Bond and lone pair domains are also observed for stishovite, despite its apparent greater closed-shell character.^{30,50} Also, it is unclear what significance should be attached to the large net charge conferred on the Si atom and the nature of the Si–O bond, given that the charges conferred on the P and S atoms are both larger and that conferred on Al is smaller, other than that the bond is an intermediate interaction.

An examination of the Si–O bond in terms of the $G(\mathbf{r}_c)/\rho(\mathbf{r}_c)$ ratio indicates that the character of the interaction is not fixed but that it depends on $\rho(\mathbf{r}_c)$, ν_{Si} , and $H(\mathbf{r}_c)$; the smaller the value of ν_{Si} , the greater the accumulation of electron density at the bcp, the more negative the value of $H(\mathbf{r}_c)$, and the more shared the interaction. The categorization of M–O bond data in terms of $G(\mathbf{r}_c)/\rho(\mathbf{r}_c)$ versus $H(\mathbf{r}_c)/\rho(\mathbf{r}_c)$ ratios also indicates that the Si–O bond is intermediate in character between the Al–O and P–O bonds, in agreement with Pauling's classic classification of the bonded interaction.^{17,18} The similarity of the bond critical point and local energy density properties of the electron density distributions displayed by silicates such as quartz and small representative molecules indicates that the bond has a shared component and behaves as if governed by short ranged molecular-like forces rather than by long range forces typically associated with ionic crystals with highly charged atoms.

Finally, the similarity of the bond lengths and angles displayed by the molecules and the silicate crystals together with the similarity of the bond critical point and local potential and kinetic energy density properties provides a basis for understanding why the force field of a molecule-like $(\text{OH})_3\text{Si}-\text{O}-\text{Si}(\text{OH})_3$ is similar to that of quartz and why it can be used successfully to generate the structures of a large number of silica polymorphs. The close similarity of the properties of the electron density distribution for the molecule and quartz also indicates that the energies of the Si–O bonded interactions are similar. Indeed, the energy of the bridging Si–O bond for quartz (465 kJ/mol) is virtually the same as that for the $(\text{OH})_3\text{Si}-\text{O}-\text{Si}(\text{OH})_3$ molecule (462 kJ/mol).⁵¹ As such, the energy involved in the formation of the bond for a quartz crystal can be expected to be similar to that for the molecule, explaining why molecular models have been useful in the derivation of the structures of a large number of silica polymorphs and in advancing our understanding of the reaction of silica with water at the atomic level.

Acknowledgment. The National Science Foundation and the U.S. Department of Energy are thanked for supporting this study in part with Grants EAR-0609885 (N.L. Ross and G.V.G.), 03ER15389 (J. D. Rimstidt and G.V.G.), and DE-FG02-97ER14751 (D.F.C.). G.V.G. thanks the Gladden Foundation for providing support for his visit to the University of Western Australia with a Gladden Senior Fellowship and thanks Virginia Tech for providing additional support for the visit.

References and Notes

- (1) Bader, R. F. W. *Atoms in Molecules*; Oxford Science Publications: Oxford, 1990.
- (2) Bader, R. F. W.; Nguyen, T. T.; Tal, Y. *Rep. Prog. Phys.* **1981**, *44*, 893.
- (3) Lasaga, A. C.; Gibbs, G. V. *Am. J. Sci.* **1990**, *290*, 263.
- (4) Xiao, Y. T.; Lasaga, A. C. *Geochim. Cosmochim. Acta* **1996**, *60*, 2283.
- (5) Xiao, Y. T.; Lasaga, A. C. *Geochim. Cosmochim. Acta* **1994**, *58*, 5379.
- (6) Filipe, M. A.; Xaio, Y.; Kubicki, J. D. *Molecular orbital modeling transition state theory in Geochemistry*; American Mineralogist: Washington, DC, 2001; Vol. 42.
- (7) Cypriak, M.; Apeloig, Y. *Organometallics* **2002**, *21*, 2165.
- (8) Boisen, M. B.; Gibbs, G. V.; Bukowinski, M. S. T. *Phys. Chem. Miner.* **1994**, *21*, 269.
- (9) Boisen, M. B., Jr.; Gibbs, G. V.; O'Keeffe, M.; Bartelmehs, K. L. *Microporous Mesoporous Mater.* **1999**, *29*, 219.
- (10) Gibbs, G. V. *Am. Mineral.* **1982**, *67*, 421.
- (11) Tossell, J. A.; Vaughan, D. J. *Theoretical Geochemistry: Applications of Quantum Mechanics in the Earth and Mineral Sciences*; Oxford University Press, Inc.: Oxford, 1992.
- (12) Mooser, E.; Pearson, W. B. *Acta Crystallogr.* **1959**, *12*, 1015.
- (13) Phillips, J. C. *Rev. Mod. Phys.* **1970**, *42*, 317.
- (14) Brownlow, A. H. *Geochemistry*; Prentice Hall, Inc.: Upper Saddle River, NJ, 1996.
- (15) Cohen, R. E. *SILICA*; Mineralogical Society: Washington, DC, 1994; Vol. 29.
- (16) Gillespie, R. J.; Johnson, S. A. *Inorg. Chem.* **1997**, *36*, 3031.
- (17) Pauling, L. *The Nature of the Chemical Bond*; Cornell University Press: Ithaca, NY, 1939.
- (18) Gibbs, G. V.; Rosso, K. M.; Teter, D. M.; Boisen, M. B., Jr.; Bukowinski, M. S. T. *J. Mol. Struct.* **1999**, *485–486*, 13.
- (19) Stewart, R. F.; Whitehead, M. A.; Donnay, G. *Am. Mineral.* **1980**, *65*, 324.
- (20) Tsirelson, V. G.; Evdokimova, O. A.; Belokoneva, E. L.; Urusov, V. S. *Phys. Chem. Miner.* **1990**, *17*, 275.
- (21) Harrison, W. A. Is silicon dioxide covalent or ionic? In *The Physics of SiO₂ and its Interfaces*; Pantelides, S. T., Ed.; Pergamon Press: New York, 1978; Ch. 2, pp 105.
- (22) Bader, R. F. W. *J. Phys. Chem. A* **1998**, *102*, 7314.
- (23) Gibbs, G. V.; Boisen, M. B.; Beverly, L. L.; Rosso, K. M. A computational quantum chemical study of the bonded interactions in earth materials and structurally and chemically related molecules. In *Molecular Modeling Theory: Applications in the Geosciences*; Cygan, R. T., Kubicki, J. D., Eds.; Mineralogical Society of America: Washington, DC, 2001; Vol. 42, p 345.
- (24) Bader, R. F. W.; Essen, H. *J. Chem. Phys.* **1984**, *80*, 1943.
- (25) Cremer, D.; Kraka, E. *Croat. Chem. Acta* **1984**, *57*, 1259.
- (26) Espinosa, E.; Alkorta, I.; Elguero, J.; Molins, E. *J. Chem. Phys.* **2002**, *117*, 5529.
- (27) Gibbs, G. V.; Boisen, M. B., Jr.; Hill, F. C.; Tamada, O.; Downs, R. T. *Phys. Chem. Miner.* **1998**, *25*, 574.
- (28) Hill, F. C.; Gibbs, G. V.; Boisen, M. B. *Phys. Chem. Miner.* **1997**, *24*, 582.
- (29) Gibbs, G. V.; Hill, F. C.; Boisen, M. B., Jr. *Phys. Chem. Miner.* **1997**, *24*, 167.
- (30) Kirfel, A.; Krane, H. G.; Blaha, P.; Schwarz, K.; Lippmann, T. *Acta Crystallogr., Sect. A* **2001**, *57*, 663.
- (31) Kirfel, A.; Lippmann, T.; Blaha, P.; Schwarz, K.; Cox, D. F.; Rosso, K. M.; Gibbs, G. V. *Phys. Chem. Miner.* **2005**, *32*, 301.
- (32) Zwiijnenburg, M. A.; Bromley, S. T.; van Alsenoy, C.; Maschmeyer, T. *J. Phys. Chem. A* **2002**, *106*, 12376.
- (33) Aubert, E.; Porcher, F.; Souhassou, M.; Lecomte, C. *Acta Crystallogr., Sect. B* **2003**, *59*, 687.
- (34) Jensen, F. *Introduction to Computational Chemistry*; John Wiley and Sons: New York, 1999.
- (35) Haaland, A.; Helgaker, T. U.; Ruud, K.; Shorokhov, D. J. *J. Chem. Educ.* **2000**, *77*, 1076.
- (36) De Proft, F.; Van Alsenoy, C.; Peeters, A.; Langenaeker, W.; Geerlings, P. *J. Comput. Chem.* **2002**, *23*, 1198.

- (37) Brom, J. M.; Schmitz, B. J.; Thompson, J. D.; Cramer, C. J.; Truhlar, D. G. *J. Phys. Chem. A* **2003**, *107*, 6483.
- (38) Bader, R. F. W.; Matta, C. F. *J. Phys. Chem. A* **2004**, *108*, 8385.
- (39) Guerra, C. F.; Handgraaf, J. W.; Baerends, E. J.; Bickelhaupt, F. M. *J. Comput. Chem.* **2004**, *25*, 189.
- (40) Gibbs, G. V.; Cox, D. F.; Crawford, T. D.; Rosso, K. M.; Ross, N. L.; Downs, R. T. *J. Chem. Phys.* **2006**, *124*.
- (41) Saunders, V. R.; Dovesi, R.; Roetti, C.; Causa, M.; Harrison, N. M.; Orlando, R.; Apra, E. *CRYSTAL98 User's Manual*; University of Torino: Torino, Italy, 1998.
- (42) Gatti, C. *TOPOND96 User's Manual*; CNR-CSR SRC: Milan, Italy, 1997.
- (43) Gibbs, G. V.; Whitten, A. E.; Spackman, M. A.; Stimpfl, M.; Downs, R. T.; Carducci, M. D. *J. Phys. Chem. B* **2003**, *107*, 12996.
- (44) Pauling, L. *J. Am. Chem. Soc.* **1929**, *51*, 1010.
- (45) Stewart, R. F.; Spackman, M. A. Charge density distributions. In *Structure and Bonding in Crystals*; O'Keeffe, M., Navrotsky, A., Eds.; Academic Press: New York, 1981; Vol. 1, p 279.
- (46) Almenningen, A.; Bastiansen, O.; Ewing, V.; Hedberg, K.; Traetteberg, M. *Acta Chem. Scand.* **1963**, *17*, 2455.
- (47) Barrow, M. J.; Ebsworth, E. A. V.; Harding, M. M. *Acta Crystallogr., Sect. B* **1979**, *35*, 2093.
- (48) Gibbs, G. V.; Spackman, M. A.; Jayatilaka, D.; Rosso, K. M.; Cox, D. F. *J. Phys. Chem. A*, in press.
- (49) Gibbs, G. V.; Cox, D. F.; Ross, N. L.; Crawford, T. D.; Burt, J. B.; Rosso, K. M. *Phys. Chem. Miner.* **2005**, *32*, 208.
- (50) Gibbs, G. V.; Cox, D. F.; Ross, N. L. *Phys. Chem. Miner.* **2004**, *31*, 232.
- (51) O'Keeffe, M., personal communication, 1983.